Study of Amplitude Control and Dynamical Behaviors of a Memristive Band Pass Filter Circuit

Zbigniew Galias
AGH University of Science and Technology
Department of Electrical Engineering
al. Mickiewicza 30, 30–059 Kraków, Poland
Email: galias@agh.edu.pl

***Abstract*—The existence of partial and total amplitude control in a band pass filter circuit with a memristor is explained theoretically and confirmed in simulations. A linear change of coordinates is derived to develop a simple three-parameter model of the circuit. Dynamical phenomena observed in the resulting dynamical system are analyzed.**

I. Introduction

The existence of nonlinear circuit elements with resistance depending on the history of current flowing through the element or the voltage across the element has been postulated in [1]. The first memristor nano-device was reported in [2]. Since then memristors have received significant attention due to a number of possible applications including large capacity non-volatile memories and neuromorphic systems.

Understanding the dynamics of circuits containing memristors is a key step in the design of memristor-based networks [3], [4], [5], [6]. A considerable research effort has been devoted to studying dynamical phenomena observed in memristor-based oscillators. In most cases these oscillators contain memristors which are built using discrete components to mimic theoretical characteristics of ideal or generalized memristors. A memristor emulator imitating the behavior of a TiO_2 memristor is presented in [7]. A floating analog memristor emulator circuit is proposed in [8]. A four dimensional memristor based chaotic circuit obtained by replacing the nonlinear element in the Chua's circuit with a memristor is studied in [3], [9]. The simplest chaotic memristor-based circuit containing an inductor, a capacitor and a memristor connected in series is studied in [10]. Further analysis of this circuit is carried out in [11] and in [12]. Dynamical phenomena in a floating memristor emulator based relaxation oscillator are analyzed in [13]. Memristive diode bridge with LCR filter is studied in [14]. Chaotic behaviors in a memristive Sallen-Key low pass filter are investigated in [15].

A simple third-order memristive band pass filter circuit is introduced [16]. The authors carry out an analysis of its equilibria and their stability, construct bifurcation diagrams and observe the phenomenon of amplitude control. In this work, the analysis of this system is continued. The mechanism of partial amplitude control is fully explained. Additionally, the property of total amplitude control is theoretically derived and confirmed in simulations. Using an appropriate linear change of variables a simple model of the circuit is constructed. The number of parameter in this model is reduced to three which considerably simplifies characterization of dynamical phenomena in the circuit. Analysis of the dynamics of the three-parameter model is carried out.

II. Third Order Memristive Band Pass Filter Circuit

The memristive band pass filter circuit [16] is shown in Fig. 1. It is built using an op-amp, two capacitors, three resistors and a memristor belonging to the class of generalized voltage controlled memristors [17]. The dynamics of the memristor is defined by

$$i_1 = R_c^{-1}(1 - g v_0^2) v_1 \tag{1}$$

$$\dot{v}_0 = -(R_b C_0)^{-1} v_0 - (R_a C_0)^{-1} v, \tag{2}$$

where i_1, v_1, and v_0 are the memristor's current, voltage, and internal variable, respectively. An implementation of this memristor using two op-amps, three resistors, one capacitor, and two multipliers is described in [16].

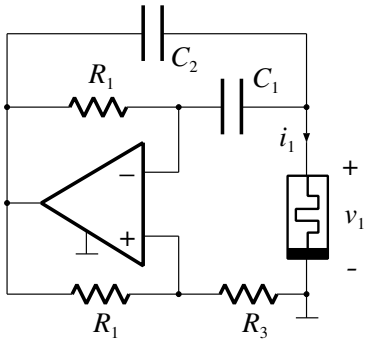

Fig. 1. The memristive band pass filter circuit.

The dynamics of the circuit presented in Fig. 1 is defined by the following system of differential equations

$$\begin{aligned}
\dot{v}_0 &= -(R_b C_0)^{-1} v_0 - (R_a C_0)^{-1} v_1, \\
\dot{v}_1 &= (1 - g v_0^2)((k-1) R_c C_2)^{-1} v_1 - R_1^{-1}(C_1^{-1} + k^{-1} C_2^{-1}) v_2, \\
\dot{v}_2 &= k(1 - g v_0^2)((k-1) R_c C_2)^{-1} v_1 - R_1^{-1}(C_1^{-1} + C_2^{-1}) v_2,
\end{aligned} \tag{3}$$

where v_1 is the voltage across the memristor, v_2 is the voltage between the ground and the output of the operational amplifier, and $k = 1 + R_2/R_3$.

Using the notation $x = v_0$, $y = v_1$, $z = v_2$, rescaling time $\tau = t/(R_1C_1)$, and defining parameters $\alpha = C_2/C_1$, $\delta = (R_1C_2)/(R_bC_0)$, $\varrho = (R_1C_2)/(R_aC_0)$, $\varepsilon = R_1/R_c$ the circuit equations can be rewritten in the dimensionless form as

$$\begin{aligned} \dot{x} &= -\delta x - \varrho y, \\ \dot{y} &= \varepsilon(1 - gx^2)(k-1)^{-1}y - (\alpha + k^{-1})z, \\ \dot{z} &= k\varepsilon(1 - gx^2)(k-1)^{-1}y - (\alpha + 1)z, \end{aligned} \tag{4}$$

Behavior of the system depends on six parameters: δ, ϱ, g, k, ε and α. In [16], the authors assume that $C_1 = C_2$. Under this assumption the parameter α is equal to 1, and the number of parameters is reduced to five. Analysis of the system (4) is carried out in [16] for the case in which four parameters are fixed $\alpha = 1$, $\varepsilon = 500/3$, $g = 0.1$, $k = 21$ and the parameters δ and ϱ are varied. Bifurcation diagrams are constructed and Lyapunov exponents are computed.

In [16], the authors compute fixed points and characteristic equations of Jacobian matrices of (4) at fixed points finding out that the characteristic equations do not depend on the parameter ϱ. They conclude that it follows that "the dynamical characteristic of system (4) has nothing to do with the parameter ϱ". This explanation is not valid. Jacobian matrices at fixed points define dynamical behaviors only in fixed points' neighborhoods. Properties of the global dynamics of the system cannot be concluded from the analysis of local behavior around fixed points alone. The authors notice that when other parameters are fixed changing the parameter ϱ rescales attractors in such a way that amplitudes of variables y and z are proportional to ϱ, while the amplitude of x does not change. They are however not able to explain this phenomenon and write "However, if the transformation $(x, y, z) \mapsto (x, y/\varrho, z/\varrho)$ is performed, the algebraic system structure will change".

III. Amplitude Control Mechanisms

In this section, we explain the phenomenon of variables' rescaling. It will be shown that rescaling variables in a proper way produces systems with different values of ϱ and other parameters unchanged. We also show that the system has a property of total amplitude control, in which all variables can be rescaled by the modification of a circuit's parameter.

First, let us notice that introducing the variable change $(x, y, z) \mapsto (x, \eta y, \eta z)$ converts (4) to the following dynamical system

$$\begin{aligned} \dot{x} &= -\delta x - \eta^{-1}\varrho y, \\ \dot{y} &= \varepsilon(1 - gx^2)(k-1)^{-1}y - (\alpha + k^{-1})z, \\ \dot{z} &= k\varepsilon(1 - gx^2)(k-1)^{-1}y - (\alpha + 1)z. \end{aligned} \tag{5}$$

The only change is in the coefficient at the y variable in the first equation. This coefficient changes from ϱ to $\eta^{-1}\varrho$. It follows that two systems (4) with different values of parameter ϱ are equivalent from the dynamical point of view. More precisely, the system (4) with parameter ϱ_1 is converted to the system with parameter ϱ_2 if the transformation $(x, y, z) \mapsto (x, \varrho_1\varrho_2^{-1}y, \varrho_1\varrho_2^{-1}z)$ is applied. Modifying the parameter ϱ is equivalent to appropriate rescaling of variables y and z while the variable x is not changed. The parameter ϱ can be used for partial amplitude control (PAC), where modifying one parameter of the system rescales amplitudes of selected variables, while amplitudes of other variables are not altered (compare [18]).

Now, we will show how to rescale all variables simultaneously in the system (4). Let us consider the following variable change $(x, y, z) \mapsto (sx, sy, sz)$, where s is the factor scaling proportionally all variables. Applying this coordinate change to (4) yields

$$\begin{aligned} \dot{x} &= -\delta x - \eta^{-1}\varrho y, \\ \dot{y} &= \varepsilon(1 - s^{-2}gx^2)(k-1)^{-1}y - (\alpha + k^{-1})z, \\ \dot{z} &= k\varepsilon(1 - s^{-2}gx^2)(k-1)^{-1}y - (\alpha + 1)z. \end{aligned} \tag{6}$$

Selecting the scaling factor s influences only the coefficients at x^2y in the second equation and third equations. The difference between (4) and (6) is that g is replaced by g/s^2. It follows that decreasing g by the factor s scales trajectories by the factor $\sqrt{s}$ in all variables. The amplitudes of all variables may be controlled by changing g. This is an example of the total amplitude control (TAC) (compare [18]).

Results regarding amplitude control are confirmed in simulations. Fig. 2(a) shows a trajectory of the system (4) with parameters $\delta = 8$, $\varrho = 80$, $\varepsilon = 500/3$, $g = 0.1$, $k = 21$, and $\alpha = 1$ with the initial condition $(x_0, y_0, z_0) = (0.1, 0, 0.1)$. Results of partial amplitude control are shown in Fig. 2(b), where ϱ is decreased two times and the initial condition is rescaled in the y and z variables $(x_0, y_0, z_0) = (0.1, 0, 0.2)$. One can see that the plot is the same as in Fig. 2(a) with the only difference in the amplitude of the y variable, which is two times larger. Similarly, the amplitude of the z variable is increased two times. Results of total amplitude control are shown in Fig. 2(c), where g is increased four times and the initial condition is rescaled in all variables to $(x_0, y_0, z_0) = (0.05, 0, 0.05)$. As a result of the total amplitude control amplitudes of all variables are decreased two times. This is consistent the with results of theoretical analysis in which we showed that the scaling factor of the amplitudes is inversely proportional to the square of the scaling factor of g. Independent rescaling of the amplitude of the x variable can be achieved by changing both ϱ and g. This is illustrated in Fig. 2(d), where ϱ is decreased two times, g is increased four times when compared to the first case, and the initial condition is rescaled in the x variable to $(x_0, y_0, z_0) = (0.05, 0, 0.1)$. As a result in this case the amplitude of x is decreased two times, while the amplitudes of y and z are unaltered.

Partial and total amplitude control mechanisms (PAC and TAC) can be observed for systems with no constant terms in the right hand side of the ordinary differential equations defining the system. Since a linear change of coordinates does not change the Lyapunov spectrum it is clear that the Lyapunov exponent spectrum is not altered by changing ϱ and g.

Amplitude control may be useful in potential applications of the circuit. The parameter ϱ is inversely proportional to R_a.

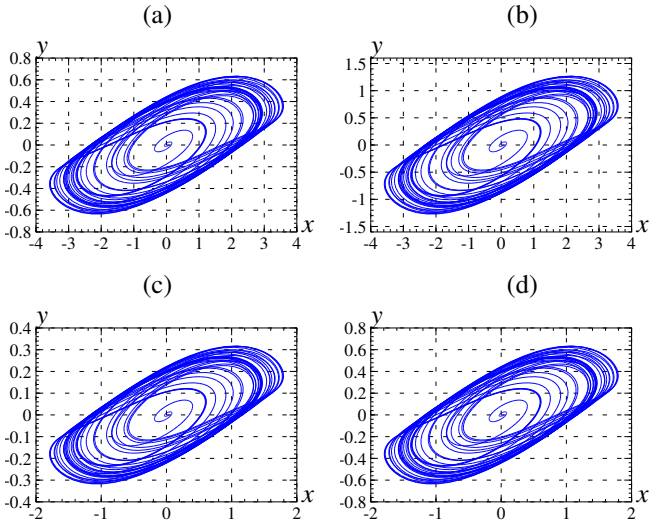

Fig. 2. Trajectories of (4) with $\delta = 8$, $\varepsilon = 500/3$, $k = 21$, and $\alpha = 1$; (a) $\varrho = 80$, $g = 0.1$, (b) $\varrho = 40$, $g = 0.1$, (c) $\varrho = 80$, $g = 0.4$, (d) $\varrho = 40$, $g = 0.4$.

Moreover, the parameter R_a is not present in definitions of δ, ε, k, and α. Hence, as noticed in [16], the amplitudes of signals generated by the circuit can be adjusted by a potentiometer at the element R_a. Changing R_a causes partial amplitude control regarding voltages v_1 and v_2. Total amplitude control resulting in scaling all voltages v_0, v_1, and v_2 is achieved by modifying the parameter g of the memristor.

IV. A Three Parameter Model of the Circuit

From the discussion presented in the previous section it follows that systems (4) with different values of parameter ϱ are equivalent from the dynamical point of view (Lyapunov spectrum is the same, solutions and attractors are simply rescaled). Hence, it is sufficient to investigate behaviors of the system for a single value of parameter ϱ, for example $\varrho = 1$. Results for other values are the same with the only difference that trajectories are rescaled. A similar observation is valid for the parameter g. Hence, we can eliminate two parameters of the system by a linear change of coordinates (4). Yet another parameter can be eliminated by using an appropriate time rescaling.

Below, we derive a linear transformation reducing the number of parameters to three and simplifying differential equations defining the dynamical system so that it contains a single nonlinear term. Let us define new variables $x = -v_0/s$, $y = v_1 R_b/(sR_a)$, $w = v_2 R_b/(skR_a)$, $\tau = t/(R_b C_0)$, where s is the scaling factor. The value of s will be selected later. In these new variables the dynamical system (3) can be rewritten as

$$\begin{aligned}
\frac{\mathrm{d}x}{\mathrm{d}\tau} &= -x + y,\\
\frac{\mathrm{d}y}{\mathrm{d}\tau} &= \frac{R_b C_0(1 - g s^2 x^2)}{(k-1)R_c C_2} y - \frac{R_b C_0(k\alpha + 1)}{R_1 C_2} w,\\
\frac{\mathrm{d}w}{\mathrm{d}\tau} &= \frac{R_b C_0(1 - g s^2 x^2)}{(k-1)R_c C_2} y - \frac{R_b C_0(\alpha + 1)}{R_1 C_2} w.
\end{aligned} \tag{7}$$

Note that nonlinear terms in (7) are identical. This allows us to simplify the set of differential equations by eliminating one of the nonlinear terms. Let use define a new variable $z = y - w$. Equations (7) in variables (x, y, z) can be written as

$$\begin{aligned}
\dot{x} &= -x + y,\\
\dot{y} &= -ay + bz - d s^2 x^2 y,\\
\dot{z} &= c(z - y),
\end{aligned} \tag{8}$$

where $a = R_b C_0(k\alpha + 1)/(R_1 C_2) - R_b C_0/((k-1)R_c C_2)$, $b = R_b C_0(k\alpha + 1)/(R_1 C_2)$, $c = R_b C_0(k-1)/(R_1 C_1)$, and $d = g R_b C_0/((k-1)R_c C_2)$. Note that for positive R_2, R_3, R_c, C_2, R_b, C_0, and g, the parameters b, c, d and the difference $b - a$ are always positive.

Let us select the scaling factor s in such a way that the coefficient at $x^2 y$ in the second equation is equal to -1, i.e. $s = \sqrt{d^{-1}} = \sqrt{(k-1)R_c C_2/(g R_b C_0)}$. This is always possible since d is positive. For this selection, we obtain a dynamical system with three parameters

$$\begin{aligned}
\dot{x} &= -x + y,\\
\dot{y} &= -ay + bz - x^2 y,\\
\dot{z} &= c(z - y).
\end{aligned} \tag{9}$$

Reducing the number of parameters from six for the model (4) to three for the model (9) simplifies the process of studying dynamical phenomena in the system.

V. Analysis of the Three Parameter Model

In this section, we analyze dynamical phenomena in the three parameter model derived in the previous section.

Let us note that the system (9) is symmetric with respect to the transformation $(x, y, z) \mapsto (-x, -y, -z)$. It follows that if $(x(t), y(t), z(t))$ is a trajectory of (9) then also is $(-x(t), -y(t), -z(t))$. As a consequence there might exist two types of steady-state solutions: self-symmetric solutions and symmetric pairs of solutions.

Under the assumption that $(b - a)$ is positive the system possesses three equilibria $(0, 0, 0)$, and $\pm x^\star = (\pm x_1^\star, \pm x_1^\star, \pm x_1^\star)$, where $x_1^\star = \sqrt{b - a}$. Since $b - a = R_b C_0/((k-1)R_c C_2) > 0$ it follows that there are always three equilibria of the original system (3).

A bifurcation diagram of the y variable at the intersection of trajectories with the plane $x = 0$ is shown in Fig. 3.

Attractors existing for selected values of a are shown in Fig. 4. In cases when a symmetric pair of attractors coexists, attractors are plotted using different colors. For $a = 2$ there exists a stable self-symmetric periodic orbit [see Fig. 4(a)]. For $a \approx 1.995$ this orbit loses stability and a symmetric pair of stable periodic orbits is born [see Fig. 4(b)]; one of the branches can be seen in the bifurcation plot. When a is decreased this periodic orbit undergoes a period doubling bifurcation for $a \approx 1.823$ [compare Fig. 4(c)]. For $a < 1.823$, there is a sequence of period-doubling bifurcations which leads to a chaotic behavior. A symmetric pair of chaotic attractors exists roughly for $a > 1.72$. An example is shown in Fig. 4(d). At $a \approx 1.72$ chaotic attractors collide and a

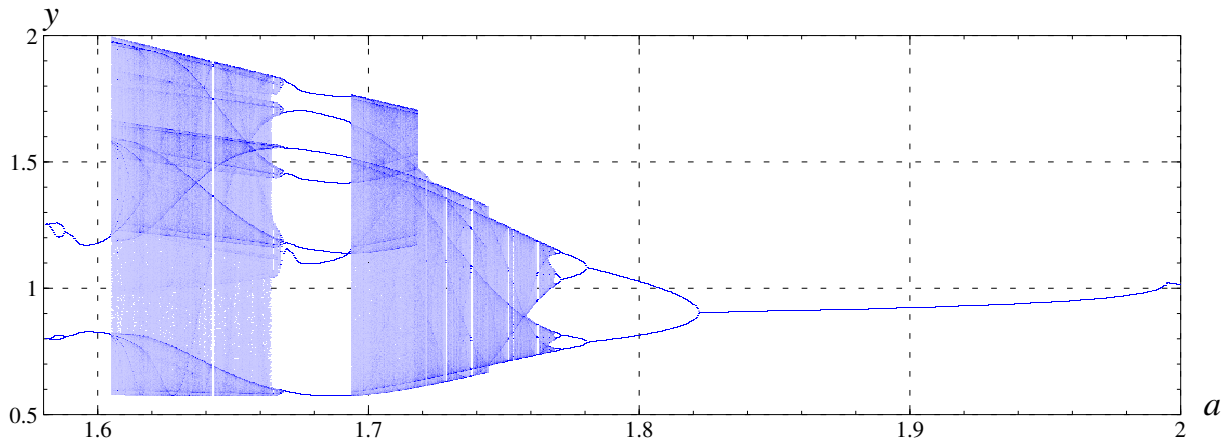

Fig. 3. Bifurcation diagram of the system (9) for $a \in [1.58, 2]$, $b = 2.75$, $c = 2.5$.

self-symmetric chaotic attractor is born [compare Fig. 4(e) and (g)]. Periodic windows exist within the chaotic region. The stable self-symmetric periodic orbit existing for $a = 1.68$ is shown in Fig. 4(f). The chaotic region exists approximately for $a > 1.605$. For $a < 1.605$ there exist two periodic attractors symmetric to each other [see Fig. 4(h)].

The existence of attractors is confirmed using interval arithmetic tools [19]. Computations in interval arithmetic are carried out in such a way that a proper rounding is used when calculating bounds of mathematical expressions. In this way results returned by a computer always enclose the true results and we can be sure that phenomena observed in simulations are not rounding error artifacts [20], [21]. The existence of attractors is studied by applying interval tools to the return map defined by the section $\{(x, y, z)\colon x = 0\}$. The return map P and its derivative are rigorously evaluated using the CAPD library [22]. The existence of all periodic attractors shown in Fig. 4 is verified using the interval Newton method [23]. In case of chaotic attractors, the existence of infinitely many periodic orbits and chaotic trajectories is confirmed using the method of covering relations [24], [21]. Computational details are skipped for the sake of brevity.

VI. Conclusions

It has been shown that a memristive band pass filter circuit possesses the total and partial amplitude control mechanisms. In the total amplitude control by changing the value of one of the circuit's parameters the amplitudes of all variables are rescaled by the same factor. In the partial amplitude control the amplitude of one of the variables remains constant while the others are rescaled by the same factor. A linear change of coordinates has been constructed in such a way that the behavior of the resulting dynamical system depends on three parameters only. Dynamical phenomena of this system has been studied.

Acknowledgments

This work was supported by the National Science Centre, Poland, grant no. 2015/17/B/ST7/03763.

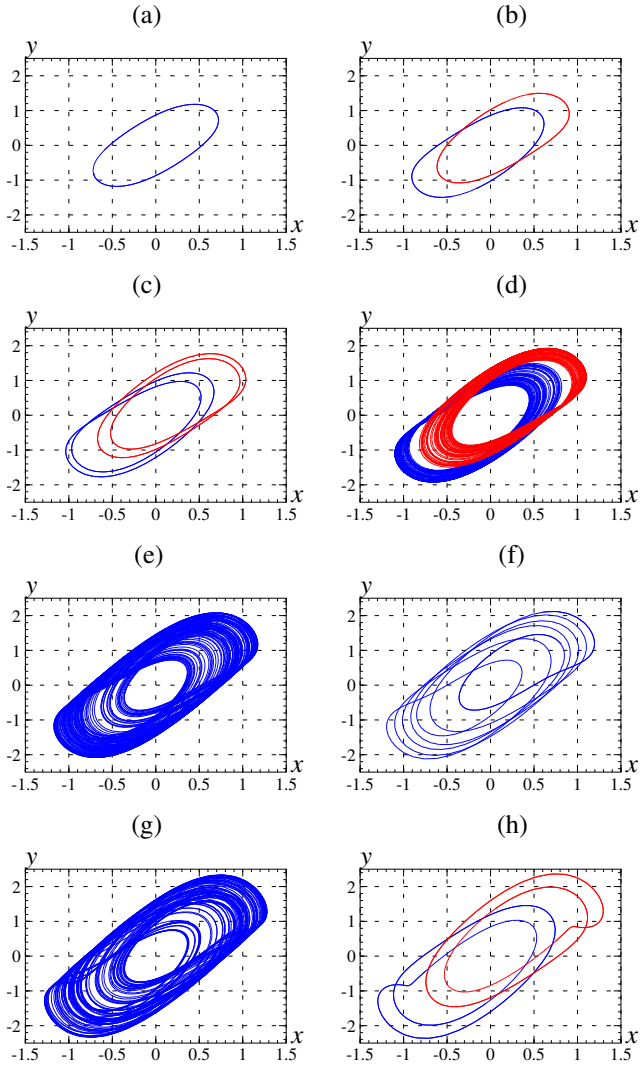

Fig. 4. Attractors existing for selected values of parameter a, $b = 2.75$, $c = 2.5$; (a) $a = 2$, (b) $a = 1.9$, (c) $a = 1.8$, (d) $a = 1.75$, (e) $a = 1.7$, (f) $a = 1.68$, (g) $a = 1.62$, (h) $a = 1.6$.

References

[1] L. O. Chua, "Memristor: The missing circuit element," *IEEE Trans. Circ. Theory*, vol. 18, no. 5, pp. 507–519, 1971.

[2] D. B. Strukov, G. S. Snider, D. R. Stewart, and R. S. Williams, "The missing memristor found," *Nature*, vol. 453, pp. 80–83, 2008.

[3] M. Itoh and L. O. Chua, "Memristor oscillators," *Int. J. Bifurcation Chaos*, vol. 18, pp. 3183–3206, 2008.

[4] F. Corinto, A. Ascoli, and M. Gilli, "Nonlinear dynamics of memristor oscillators," *IEEE Trans. Circuits Systems I*, vol. 58, no. 6, pp. 1323–1336, 2011.

[5] R. Riaza, "First order mem-circuits: Modeling, nonlinear oscillations and bifurcations," *IEEE Trans. Circuits Systems I*, vol. 60, no. 6, pp. 1570–1583, 2013.

[6] M. Itoh and L. O. Chua, "Dynamics of memristor circuits," *Int. J. Bifurcation Chaos*, vol. 24, no. 5, p. 1430015, 2014.

[7] H. Kim, M. P. Sah, C. Yang, S. Cho, and L. O. Chua, "Memristor emulator for memristor circuit applications," *IEEE Trans. Circ. Syst. I*, vol. 59, no. 10, pp. 2422–2431, 2012.

[8] C. Sánchez-López, J. Mendoza-López, M. Carrasco-Aguilar, and C. Muniz-Montero, "A floating analog memristor emulator circuit," *IEEE Trans. Circ. Syst. II*, vol. 61, no. 5, pp. 309–313, 2014.

[9] H. H. C. Iu, D. S. Yu, A. L. Fitch, V. Sreeram, and H. Chen, "Controlling chaos in a memristor based circuit using a twin-T notch filter," *IEEE Trans. Circ. Syst. I*, vol. 58, no. 6, pp. 1337–1344, 2011.

[10] B. Muthuswamy and L. Chua, "Simplest chaotic circuit," *Int. J. Bifurcation and Chaos*, vol. 20, no. 5, pp. 1567–1580, 2010.

[11] Y. Zhang and X. Zhang, "Dynamics of the Muthuswamy-Chua system," *Int. J. Bifurcation and Chaos*, vol. 23, no. 8, p. 1350136 (7 pages), 2013.

[12] Z. Galias, "Automatized search for complex symbolic dynamics with applications in the analysis of a simple memristor circuit," *Int. J. Bifurcation Chaos*, vol. 24, no. 7, p. 1450104 (11 pages), 2014.

[13] D. Yu, H. H. C. Iu, A. L. Fitch, and Y. Liang, "A floating memristor emulator based relaxation oscillator," *IEEE Trans. Circ. Syst. I*, vol. 61, no. 10, pp. 2888–2896, 2014.

[14] F. Corinto and A. Ascoli, "Memristive diode bridge with LCR filter," *Electronics Letters*, vol. 48, no. 14, pp. 824–825, 2012.

[15] B. C. Bao, P. Wu, H. Bao, M. Chen, and Q. Xu, "Chaotic bursting in memristive diode bridge-coupled Sallen-Key lowpass filter," *Electronics Letters*, vol. 53, no. 16, pp. 1104–1105, 2017.

[16] B. Bao, N. Wang, Q. Xu, H. Wu, and Y. Hu, "A simple third-order memristive band pass filter chaotic circuit," *IEEE Trans. Circ. Syst. II*, vol. 64, no. 8, pp. 997–981, 2017.

[17] L. O. Chua, "The fourth element," *Proc. IEEE*, vol. 100, no. 6, pp. 1920–1927, 2012.

[18] C. Li and J. Sprott, "Amplitude control approach for chaotic signals," *Nonlinear Dynamics*, vol. 73, no. 3, pp. 1335–1341, 2013.

[19] R. Moore, *Methods and applications of interval analysis*. Philadelphia: SIAM, 1979.

[20] R. Lozi, "Can we trust in numerical computations of chaotic solutions of dynamical systems?" in *Topology and Dynamics of Chaos*, C. Letellier and R. Gilmore, Eds. World Scientific, 2013, vol. 84, pp. 29–64.

[21] Z. Galias, "The dangers of rounding errors for simulations and analysis of nonlinear circuits and systems — and how to avoid them," *IEEE Circuits Syst. Mag.*, vol. 13, no. 3, pp. 35–52, 2013.

[22] "CAPD library," http://capd.ii.uj.edu.pl/, 2016.

[23] A. Neumaier, *Interval Methods for Systems of Equations*. Cambridge, UK: Cambridge University Press, 1990.

[24] P. Zgliczyński, "Computer assisted proof of chaos in the Rössler equations and in the Hénon map," *Nonlinearity*, vol. 10, no. 1, pp. 243–252, 1997.